

Event-Triggered Distributed Data-driven Iterative Learning Bipartite Formation Control for Unknown Nonlinear Multi-agent Systems

Huarong Zhao, Hongnian Yu, *Senior Member, IEEE*, and Li Peng

Abstract—In this study, we investigate the event-triggering time-varying trajectory bipartite formation tracking problem for a class of unknown nonaffine nonlinear discrete-time multi-agent systems (MASs). We first obtain an equivalent linear data model with a dynamic parameter of each agent by employing the pseudo partial derivative technique. Then we propose an event-triggered distributed model-free adaptive iterative learning bipartite formation control scheme by using the input/output data of MASs without employing either the plant structure or any knowledge of the dynamics. To improve the flexibility and network communication resource utilization, we construct an observer-based event-triggering mechanism with a dead-zone operator. Furthermore, we rigorously prove the convergence of the proposed algorithm, where each agent’s time-varying trajectory bipartite formation tracking error is reduced to a small range around zero. Finally, four simulation studies further validate the designed control approach’s effectiveness, demonstrating that the proposed scheme is also suitable for the homogeneous MASs to achieve time-varying trajectory bipartite formation tracking.

Index Terms—Data-driven control, multi-agent systems, bipartite formation, event-triggered control, iterative learning.

I. INTRODUCTION

THE past decades have witnessed the burgeoning development of the multi-agent systems (MASs) formation control approaches for the fact that most of these approaches apply to a variety of space missions, such as target tracking, satellite clustering, and environmental monitoring. The main task of formation control is to construct and maintain a prespecified position-orientation pattern of each agent in an alliance. A number of general schemes of formation control are studied in the literature [1]–[7]. The underactuation and high nonlinearities problems for a group of quadrotors are considered in [1] by formulating a robust formation control approach, which includes a distributed robust controller and an attitude controller to realize translational and rotational motion

control. Furthermore, external disturbances [2], [3], switching topologies [4]–[6], and communication delays [7]–[9] are extensively researched, and other interesting problems are surveyed in [10]–[12]. These demonstrate that the formation control problem is a hot research topic of MASs.

On the other hand, increasing the number of agents exposes the drawback of agents’ hardware, such as limited bandwidth and communication channels among agents. The distributed event-triggered strategies, which can ease this problem, have received much attention from scholars in recent years [13]–[19]. The objective of distributed event-triggered strategies is to formulate an appropriate event-triggered condition (ETC) and a distributed control protocol for the controlled plant. Violating the ETC will initiate the controlled system to transmit the measurement data and update the control command. On the other hand, compared with the traditional centralized manner, the distributed event-triggered methods only depend on local information exchanges among neighbors using the communication networks sharing technique. Hence, the distributed event-triggered approaches not only ensure the desired control performance but also save communication and computation resources [13]. A dynamic event-triggered communication strategy is designed in [14] for MASs to implements formation control tasks, where the parameters of ETC are dynamically adjustable according to a dynamic rule. Inspired by [14], the authors in [15] propose an event-triggered consensus control protocol for linear MASs, which can endure prolonged the minimum interevent time between two consecutive triggering instants and avoid Zeno behavior. Moreover, the authors in [16] introduce an adaptive parameter adjustment algorithm into the event-triggered control strategy to meet the time-varying formation control requirements of linear MASs. It is noted that the resource-efficient formation control for MASs is still a hot topic, and the related issues [13], [17]–[19] should be further investigated. However, all the motivated works consider the formation control for the MASs with known dynamics. In other words, most existing proposed approaches belong to the classic model-based control (MBC) domain. In practice, it is hard to obtain the plant’s accurate mathematic model for a large-scale and complicated modern practical controlled plant. Furthermore, the traditional MBC schemes cannot directly cope with the controlled systems without explicit or implicit dynamics.

To address the above modeling problems, several data-driven control (DDC) schemes have been developed, for example, model-free adaptive control (MFAC) [20]–[22], model-

Manuscript received February 02, 2021; revised July 31, 2021; revised November 26, 2021; revised March 27, 2022; accepted May 09, 2022. This work was supported by the National Natural Science Foundation of China under Grant (61873112,61802107), the Natural Science Research Project of Higher Education in Jiangsu Province under Grant 18KJB413009, Taizhou Development and Reform Commission fund project under Grant 2106-331000-04-04-295510, the China Scholarship Council under Grant 202106790082.

(Corresponding author: Li Peng)

Huarong Zhao and Li Peng are with Engineering Research Center of Internet of Things Applications Ministry of Education, Jiangnan University, Wuxi 214122, Jiangsu, China (e-mail: zhaohuarong@stu.jiangnan.edu.cn; jipengli@outlook.com).

Hongnian Yu is with the School of Engineering and the Built Environment, Edinburgh Napier University, EH10 5DT Edinburgh, UK (e-mail: h.yu@napier.ac.uk).

free adaptive iterative learning control (MFAILC) [23]–[25], virtual reference feedback tuning (VRFT) [26], [27], and reinforcement learning (RL) [28]–[30]. The DDC approaches' main characteristic is to design a controller for the controlled plant without requiring knowledge of the controlled plant structure, only utilizing the controlled system's input/output (I/O) measurement data. It is noted that MFAC, VRFT, and RL are not suitable for the controlled plant to execute repeatable or periodic tasks. However, there is a class of special production requirements that control tasks are repeatable, and operation errors should be avoided in the whole of the production process, for instance, IC welding and wafer manufacturing [31]. To the best of our knowledge, the MFAILC approach is one of the effective strategies for MASs with repeatable tasks. Since the 1980s, the iterative learning control (ILC) scheme has been extensively developed. The ILC method is initially employed to solve the formation problem in [32] for affine nonlinear MASs with a fixed communication topology. The method of [32] is extended in [33] to improve the algorithm's robustness considering the communication delays. An MFAILC method is proposed in [34] for MASs to implement time-varying trajectory consensus tracking tasks. Considering [34], MFAILC is extended to perform formation tracking tasks for MASs with switching topologies in [35]. An enhanced model-free iterative learning formation control approach is proposed in [36]. Although several ILC methods have been developed, the study for MASs with unknown nonaffine nonlinear dynamics is still open from the above analysis. Therefore, research on formation control for unknown nonaffine nonlinear MASs via the ILC scheme under repetitive circumstances is useful, which is also a motivation of our investigation.

The literature review shows that most published papers are only forced on the collaborative relationship among agents to develop consensus control or formation control approaches. However, since multi-agent systems are derived from people's systematic abstraction of group behavior, it is inevitable that agents cooperate and compete. Altafini [37] first introduces the bipartite consensus concept for the MASs with antagonistic interactions. The goal of bipartite formation is that all agents deviate into two groups, and the two groups have the same reference object except for signs. Although a few bipartite formation algorithms have been developed [38]–[41], they require an accurate mathematical model or need to establish a complex nervous network. A dynamic event triggering mechanism for linear MASs to realize bipartite output consensus control is studied in [38]. A bipartite consensus protocol is considered for the MASs with the switching topologies problem in [39]. The time-varying delay and the hybrid impulses problems for MASs to perform bipartite formation tasks are investigated in [40] and [41], respectively. Although many efforts have been made in bipartite consensus or formation methods for MASs, combining data-driven iterative learning approach to design an appropriate event-triggered controller for MASs to implement time-varying trajectory bipartite formation tracking tasks has not yet received attention. Thus, this leads to the third motivation for this article.

This paper addresses the event triggering time-varying trajectory bipartite formation tracking problem for unknown

nonaffine nonlinear detected-time MASs under the repetitive environment. The main contributions of this paper are:

- 1) Developing an equivalent linear data model with a dynamic parameter for each agent using the pseudo partial derivative technique. The developed model is also suitable for heterogeneous and time-varying parameters MASs. Compared with the MBC approaches [1]–[20], the model structure is simpler, and the computation costs are reduced.
- 2) Proposing an observer to achieve event triggering control, whose flexibility is further guaranteed by the designed dead-zone operator. We only use the I/O data to formulate the designed event-triggered distributed model-free adaptive iterative learning bipartite formation control (ET-DMFAILBFC) approach, which can reduce each agent's tracking errors to perform time-varying trajectory tracking tasks. Although several effective algorithms for the event-triggered problem are considered in [13]–[18] and [38], [39], they are dependent on accurate dynamics, which is not easy to be implemented practically.
- 3) Synthesizing elements of event triggering mechanism, iterative learning, cooperative and competitive interactions, fixed and time-varying switching topologies for unknown nonaffine nonlinear detected-time MASs to perform time-varying trajectory bipartite formation tracking tasks. To the best of our knowledge, only a small fraction of the above elements are considered in [15], [34], and [38].

The rest of this article is structured as follows. Section II introduces the signed graph theory and problem formulation. Section III presents the proposed ET-DMFAILBFC algorithm and gives rigorous mathematical proof. Section IV discusses the time-varying switching topologies problem for MASs to perform event-triggered bipartite formation tracking tasks. Several simulations are presented in Section V to further verify the designed ET-DMFAILBFC algorithm's effectiveness and practicability. Finally, Section VI presents the conclusion.

Notations: The set of real numbers, positive real numbers, positive integers, and identify matrices with arbitrary dimension are expressed by R , R^+ , Z^+ , and I , respectively. $diag(\bullet)$, $sign(\bullet)$, and $\lfloor \bullet \rfloor$ denote diagonal matrix, sign function, and the floor function, respectively. $\|\Theta\|$ stands for the Euclidean norm of vector $\Theta \in R^N$. Moreover, $k \in \{0, 1, \dots, T\}$ and $l = 0, 1, 2, \dots$ stand for time interval and iteration number, respectively.

II. PRELIMINARY AND PROBLEM FORMULATION

A. signed graph theory

This paper considers a competition communication topology of the MASs with N agents, which is denoted by a signed graph $G = (V_G, E_G, A_G)$. $V_G = \{v_1, \dots, v_N\}$, $E_G = \{(v_i, v_j) | v_i, v_j \in V_G\} \subseteq V_G \times V_G$, and $A_G = [a_{ij}] \in R^{N \times N}$ stand for nodes, edges, and the weighted adjacency matrix with $-1, 0, 1$ elements, respectively. The neighborhood of the node i is expressed by $N_i = \{j \in V_G | (j, i) \in E_G\}$, and the degree matrix of G is expressed by $D_G = diag\{d_1, \dots, d_N\}$ with $d_i = \sum_{j \in N_i} |a_{ij}|$. $L = -A_G + D_G$ stands for the Laplacian matrix of G . Generally, the virtual leader is considered as the

node 0 to be added in the graph \bar{G} . Hence, an augmentation graph $\bar{G} = (\bar{V}_G, \bar{E}_G, A_G)$ is introduced, where $\bar{V}_G = V_G \cup \{v_0\}$ and $\bar{E}_G = \bar{V}_G \times \bar{V}_G$. To describe the connecting relationship between the virtual leader and the agent i , a connecting matrix $B = \text{diag}\{b_1, \dots, b_N\}$ is defined, where $b_i = 1$ denotes that the virtual leader is directly connected with the agent i . Moreover, if the graph \bar{G} is strongly connected, the \bar{G} has a directed communication path from the virtual leader to any other agents.

In addition, the graph \bar{G} is also called structurally balanced, where the whole nodes V_G of \bar{G} can be divided into two subsets V_1 and V_2 , and F is restricted by the following conditions: 1) $V_1 \cup V_2 = V_G$ and $V_1 \cap V_2 = \emptyset$; 2) If $\forall i, j \in V_z$ with $z \in \{1, 2\}$, $a_{ij} \in \{0, 1\}$; 3) If $\forall i \in V_z$ and $j \in V_q$ with $z \neq q$, ($z, q \in \{1, 2\}$), $a_{ij} \in \{-1, 0\}$. If $(v_j, v_i) \notin E_G$ or $i = j$, $a_{ij} = 0$. If $v_j \in V_q$, $v_i \in V_z$, $z \neq q$, and $(v_j, v_i) \in E_G$, $a_{ij} = -1$. A grouping matrix $s = \text{diag}(s_1, \dots, s_N)$ is often employed to describe the relationship between agents and groups. If the agent $i \in V_1$, $s_i = 1$; otherwise, $s_i = -1$.

In order to describe the time-varying switching topologies, an enhanced graph $\bar{G}(k) = (\bar{V}_G(k), \bar{E}_G(k), A_G(k))$ is introduced, and all of the possible topologies of MASs are described by $\bar{G}(k) = \bar{G}^p = \{\bar{G}^1, \dots, \bar{G}^\kappa\}$, $\kappa \in Z^+$. The Laplacian matrix of $\bar{G}(k)$ can be calculated by $L(k) = -A_G(k) + D_G(k)$, where $A_G(k) = [a_{ij}^p(k)] \in R^{N \times N}$ and $D_G(k) = \text{diag}\{d_1^p(k), \dots, d_N^p(k)\}$. Moreover, the corresponding connecting matrix and grouping matrix become $B(k) = \text{diag}\{b_1^p(k), \dots, b_N^p(k)\}$ and $s(k) = \text{diag}\{s_1^p(k), \dots, s_N^p(k)\}$, respectively. Furthermore, for facility of analysis, S_n is often defined as the set of agents.

B. Problem Formulation

In this paper, we study a class of unknown non-affine SISO (single-input-single-output) nonlinear discrete-time MASs with N agents. The i th agent's nonlinear dynamics is considered as below.

$$\begin{aligned} y_i(l, k+1) &= f_i(y_i(l, k), \dots, y_i(l, k-n_y), \\ &u_i(l, k), \dots, u_i(l, k-n_u)) \end{aligned} \quad (1)$$

where $n_y \in Z^+$ and $n_u \in Z^+$ are unknown. $u_i(l, k) \in R$ represents the control input of the agent i with $i \in S_n$, and the corresponding output is expressed by $y_i(l, k) \in R$. $f_i(\bullet)$ denotes an unknown nonlinear function, and $\bar{G} = (\bar{V}_G, \bar{E}_G, A_G)$ denotes the communication topology among agents.

To facilitate the analysis, we introduce two assumptions of agents' dynamic below.

Assumption 1 ([34]): $f_i(\bullet)$ is a continuously differentiable equation for $u_i(l, k)$.

Assumption 2 ([35]): As the nonlinear dynamics (1) satisfies the generalized Lipschitz condition along the iteration axis, $|\Delta y_i(l, k+1)| \leq r |\Delta u_i(l, k)|$ holds for all k and l , where $r \in R^+$ is a constant, $\Delta y_i(l, k+1) = y_i(l, k+1) - y_i(l-1, k+1)$, $\Delta u_i(l, k) = u_i(l, k) - u_i(l-1, k) \neq 0$, and $|\Delta u_i(l, k)|$ is bounded by $a \in R^+$.

Remark 1: Assumption 1 is a basic condition for developing a control protocol. Assumption 2 implies that we can always find a value of r to represent the relationship between the

changing rate of input and output at any point, and limit input leads to limit output applying the principle of systems energy conservation. More details can be found in [34] and [35].

Lemma 1 ([23], [35], [42]): If the nonlinear dynamics (1) meets the condition described in Assumptions 1 and 2, an equivalent linear data model can be obtained below.

$$\Delta y_i(l, k+1) = \Gamma_i(l, k) \Delta u_i(l, k) \quad (2)$$

where $\Gamma_i(l, k)$ represents an iteration-dependent and time-varying parameter, which is called pseudo-partial-derivative (PPD) with $|\Gamma_i(l, k)| \leq r$, and input gain $|\Delta u_i(l, k)| \leq a$, for all k and l . Moreover, r and a are small positive constant, and the details of them are discussed in [23], [35] and [42].

Next, the two fundamental Assumptions of the bipartite formation control are presented below.

Assumption 3 ([25], [34]): For all k and l , $\Gamma_i(l, k)$ meets that $\Gamma_i(l, k) > \iota > 0$ ($\Gamma_i(l, k) < -\iota < 0$), $i \in S_n$, where $\iota \in R^+$ is arbitrarily small. Generally, suppose that $\Gamma_i(l, k) > \iota > 0$.

Assumption 4: The communication topology \bar{G} or \bar{G}^p is structurally balanced. Meanwhile, \bar{G} or \bar{G}^p is strongly connected. In other words, there is a directed communication path between each agent and the virtual leader.

Lemma 2 ([35]): If \bar{G} or \bar{G}^p satisfies Assumption 4, the $L + B$ of \bar{G} or $L(k) + B(k)$ of \bar{G}^p is a positive definite and irreducible matrix.

Definition 1: The goal of the bipartite formation control scheme is to formulate an appropriate control protocol $u_i(l, k)$, which can generate a predicted formation and maintain it. For each agent i , the following conditions are satisfied.

$$\lim_{l \rightarrow \infty} (y_i(l, k) - y_0(l, k)) = g_i(l, k) \quad (3)$$

where the agent i belongs to V_1 . If the agent i belongs to V_2 ,

$$\lim_{l \rightarrow \infty} (y_i(l, k) + y_0(l, k)) = g_i(l, k) \quad (4)$$

where $g_i(l, k)$ denotes desired gaps from the agent i to the virtual leader, and $y_0(l, k)$ is the position of the virtual leader.

In this paper, a grouping matrix s is introduced to describe the cooperation relationships among agents, where $s = \text{diag}(s_1, s_2, \dots, s_N)$ and $s_i \in \{-1, 1\}$. If the agent i belongs to V_1 , $s_i = 1$; otherwise, $s_i = -1$. Hence, the conditions (3) and (4) can be expressed as

$$\lim_{l \rightarrow \infty} (y_i(l, k) - s_i y_0(l, k)) = g_i(l, k) \quad (5)$$

Define $\xi_i(l, k)$ as the local error of the agent i at the l th iteration as below:

$$\begin{aligned} \xi_i(l, k) &= \sum_{j \in N_i} (a_{ij} \tilde{y}_j(l, k) - |a_{ij}| \tilde{y}_i(l, k)) \\ &+ b_i (s_i y_0(l, k) - \tilde{y}_i(l, k)) \end{aligned} \quad (6)$$

where the value of b_i is dependent on the connected relationship between the virtual leader and the agent i , that is, if the agent i is directly connected with the virtual leader, $b_i = 1$; otherwise, $b_i = 0$. Here, $\tilde{y}_i(l, k) = \hat{y}_i(l, k) - g_i(l, k)$, where $\hat{y}_i(l, k)$ is the estimation of $y_i(l, k)$. Moreover, let $\tilde{e}_i(l, k) = s_i y_0(l, k) - \tilde{y}_i(l, k)$ denotes the bipartite formation tracking

Case2: $Q(l-1, k)=0$. In this case, (8) becomes $\hat{\Gamma}_i(l, k) = \hat{\Gamma}_i(l-1, k)$. Then, according to (10), we have $\hat{\Gamma}_i(l, k) = \hat{\Gamma}_i(l-1, k) = \dots = \hat{\Gamma}_i(1, k)$. Thus, $\hat{\Gamma}_i(l, k)$ is bounded.

Hence, there is a constant \hat{r} , which is the upper bound of $\hat{\Gamma}_i(l, k)$. ■

B. Distributed event-triggered mechanism

An output observer is designed as follows.

$$\begin{aligned} \hat{y}_i(l, k+1) &= \hat{y}_i(l-1, k+1) + \hat{\Gamma}_i(l, k)\Delta\tilde{u}_i(l, k) \\ &+ \chi\tilde{\varepsilon}_{e_i}(l-1, k+1) \end{aligned} \quad (15)$$

where $\hat{y}_i(l, k+1)$ represents the output of observer i at time interval k . Moreover, χ represents the feedback gain, which is discussed later. $\Delta\tilde{u}_i(l, k)$ and $\tilde{\varepsilon}_{e_i}(l-1, k+1)$ are defined as

$$\Delta\tilde{u}_i(l, k) = \Delta u_i(l, k_i), \quad k_i \leq k < k_{i+1} \quad (16)$$

$$\tilde{\varepsilon}_{e_i}(l-1, k+1) = \hat{y}_i(l-1, k+1) - \tilde{y}_i(l-1, k+1) \quad (17)$$

where $\tilde{y}_i(l-1, k+1)$ is designed as

$$\tilde{y}_i(l-1, k+1) = y_i(l-1, k_i), \quad k_i \leq k+1 < k_{i+1} \quad (18)$$

From (16) and (18), we can find that $\Delta\tilde{u}_i(l, k)$ and $\tilde{y}_i(l-1, k+1)$ maintain the last event-triggered instant's values until the next event-triggered instant. Moreover, the event-triggered incremental input error $\varepsilon_i(l, k)$ is described by

$$\varepsilon_i(l, k) = \Delta u_i(l, k) - \Delta\tilde{u}_i(l, k) \quad (19)$$

Moreover, the observer-based output estimation error is described as

$$\varepsilon_{e_i}(l, k+1) = \hat{y}_i(l, k+1) - y_i(l, k+1) \quad (20)$$

Then, the event-triggered condition is defined as

$$\begin{aligned} \eta(|\varepsilon_i(l, k)|) &> \sqrt{\frac{u(1-4(1+\chi)^2)}{4\hat{r}^2}} |\varepsilon_{e_i}(l-1, k+1)| \\ &\text{or } k - k_i \geq \bar{k} \end{aligned} \quad (21)$$

where $\bar{k} \in Z^+$ and \hat{r} is the bound of $\hat{\Gamma}_i(l, k)$. Moreover, u and χ are constants that are discussed in Theorem 2, and $\eta(\bullet)$ denotes the dead-zone operator, which is designed as

$$\eta(|\varepsilon_i(l, k)|) = \begin{cases} |\varepsilon_i(l, k)|, & |\varepsilon_{e_i}(l-1, k+1)| > \tau \\ 0, & \text{otherwise} \end{cases} \quad (22)$$

where τ is the bound of $\varepsilon_{e_i}(l, k)$ and it will be discussed later.

Remark 4: It is noted that (22) starts to consider the changing rate of control input $u_i(l, k)$, only when the output estimation error $|\varepsilon_{e_i}(l-1, k+1)|$ exceeds the threshold τ . When the changing rate of control input exceeds the stability condition (21), the control input $u_i(l, k)$ will start to be updated. The second event-triggered condition $k - k_i \geq \bar{k}$ is introduced to check whether something wrong with the trigger. Moreover, the dead-zone operator can effectively improve the flexibility of the proposed method and further avoid Zeno-like behavior as [43].

Theorem 2: When Equation (1) satisfies Assumptions 1-3, $\Gamma_i(l, k)$ is estimated by laws (8)-(10), and the event-triggering condition is selected as (21), then $\varepsilon_{e_i}(l, k)$ is bounded.

Proof: Substituting (2), (15), and (17) into (20) leads to the following equation

$$\begin{aligned} \varepsilon_{e_i}(l, k+1) &= (1+\chi)\varepsilon_{e_i}(l-1, k+1) + \chi E_i(l-1, k+1) \\ &- \varepsilon_i(l, k)\hat{\Gamma}_i(l, k) + \tilde{\Gamma}_i(l, k)\Delta u_i(l, k) \end{aligned} \quad (23)$$

where $E_i(l-1, k+1) = y_i(l-1, k+1) - \tilde{y}_i(l-1, k+1)$. Since $\Delta y_i(l, k+1) = \Gamma_i(l, k)\Delta u_i(l, k)$, $0 < \Gamma_i(l, k) < r$, and $|\Delta u_i(l, k)| < a$, $\Delta y_i(l, k)$ is bounded. Hence, existing a constant α can guarantee that $E_i(l-1, k+1) < \alpha$.

Then, the boundedness of $\varepsilon_{e_i}(l, k)$ is considered in two cases. One is $k=k_i$, and other is $k_i < k < k_{i+1}$.

Case1: $k=k_i$. We have $\Delta\tilde{u}_i(l, k) - \Delta u_i(l, k) = 0$, $\tilde{y}_i(l-1, k+1) = y_i(l-1, k+1)$, and $E_i(l-1, k+1) = 0$. Hence, (23) can be rewritten as below.

$$\begin{aligned} \varepsilon_{e_i}(l, k+1) &= (1+\chi)\varepsilon_{e_i}(l-1, k+1) \\ &+ \tilde{\Gamma}_i(l, k)\Delta u_i(l, k) \end{aligned} \quad (24)$$

Let's define the following Lyapunov function

$$V_i(l, k) = \varepsilon_{e_i}^2(l, k) \quad (25)$$

Substituting (24) into (25) gives

$$\Delta V_i(l, k+1) \leq \varphi - (1-2(1+\chi)^2)\varepsilon_{e_i}^2(l-1, k+1) \quad (26)$$

where $\varphi = 2\left(\frac{r}{1-q_1}\right)^2 a^2$. Therefore, in this case, the stability condition is

$$|\varepsilon_{e_i}(l-1, k+1)| > \sqrt{\frac{\varphi}{1-2(1+\chi)^2}} = \tau \quad (27)$$

Case2: $k_i < k < k_{i+1}$. From (19), (23), (25), and Lemma 1, we have

$$\Delta V_i(l, k+1) \leq \theta - (1-u)(1-4(1+\chi)^2)\varepsilon_{e_i}^2(l-1, k+1) \quad (28)$$

where $\theta \geq 4\chi^2\alpha^2 + 4\hat{r}^2a^2$, $0 < u < 1$ and $u(1-4(1+\chi)^2)\varepsilon_{e_i}^2(l-1, k+1) \geq 4\hat{r}^2\varepsilon_i^2(l, k)$. Then, the condition of event-triggered control can be obtained as

$$|\varepsilon_i(l, k)| \leq \sqrt{\frac{u(1-4(1+\chi)^2)}{4\hat{r}^2}} |\varepsilon_{e_i}(l-1, k+1)| \quad (29)$$

According to (25) and (28), we obtain the following inequality.

$$\begin{aligned} V_i(l, k+1) &\leq (1-(1-u)(1-4(1+\chi)^2))^{l-1} V_i(1, k+1) \\ &+ \frac{\theta(1-(1-(1-u)(1-4(1+\chi)^2))^{l-1})}{1-(1-(1-u)(1-4(1+\chi)^2))} \end{aligned} \quad (30)$$

If $0 < 1-(1-u)(1-4(1+\chi)^2) < 1$, we have

$$\lim_{l \rightarrow \infty} |V_i(l, k+1)| = \frac{\theta}{1-(1-(1-u)(1-4(1+\chi)^2))}$$

Thus, we have that $-1.5 < \chi < -0.5$. It ensures the boundedness of $\varepsilon_{e_i}(l, k)$. ■

C. Distributed event-triggered bipartite formation

In this part, an event-triggered distributed data-driven iterative learning bipartite formation control approach is developed. The convergence of the bipartite formation tracking error is analyzed. Firstly, the event-triggered distributed data-driven controller is designed as below.

$$u_i(l, k) = u_i(l-1, k) + Q(l-1, k) \frac{\beta \hat{\Gamma}_i(l, k)}{\lambda + |\hat{\Gamma}_i(l, k)|^2} \quad (31)$$

$$\times \xi_i(l-1, k+1)$$

where $\xi_i(l-1, k+1)$ is the local error, which is given in (6). $Q(l-1, k)$ is an index operator defined in (9). $\hat{\Gamma}_i(l, k)$ is the estimation of $\Gamma_i(l, k)$, and $\lambda > 0$ is stability factor. β is a penalty factor, which will be discussed later.

For the next analysis, we introduce the following Lemma.

Lemma 3 ([44]): For $\phi = 1, 2, \dots, i$ with $i \in Z^+$, $M(\phi)$ is an iteration varying irreducible substochastic matrix with positive diagonal entries. Then, we have

$$\|M(\phi)M(\phi-1)\cdots M(1)\| \leq \lambda$$

where $0 < \lambda < 1$ and $\phi \leq i$.

The convergence proof of the designed ET-DMFAILBFC scheme is given in Theorem 3.

Theorem 3: Considering Equation (1) restrained by Assumptions 1-3, the MASs' topology restrained by Assumption 4, the PPD estimated by (8)-(10), and employing the proposed distributed event-triggered controller (31), where the event-triggering condition satisfies (21) and the β is selected as

$$\beta < \frac{1}{\max_{i \in S_n} \sum_{j=1}^N |a_{ij}| + b_i}$$

there is a λ_{\min} with $\lambda > \lambda_{\min} > \frac{r^2}{4}$ such that $e_i(l, k)$ is bounded.

Proof: Since $\tilde{e}_i(l, k) = s_i y_0(l, k) - \tilde{y}_i(l, k)$, (6) becomes

$$\xi_i(l, k) = \sum_{j \in N_i} (a_{ij} \tilde{e}_i(l, k) - |a_{ij}| \tilde{e}_j(l, k)) + b_i \tilde{e}_i(l, k) \quad (32)$$

To facilitate the analysis, we define that

$$u(l, k) = [u_1(l, k), u_2(l, k), \dots, u_N(l, k)]^T,$$

$$\xi(l, k) = [\xi_1(l, k), \xi_2(l, k), \dots, \xi_N(l, k)]^T,$$

$$\tilde{e}(l, k) = [\tilde{e}_1(l, k), \tilde{e}_2(l, k), \dots, \tilde{e}_N(l, k)]^T,$$

$$\varepsilon_e(l, k) = [\varepsilon_{e1}(l, k), \varepsilon_{e2}(l, k), \dots, \varepsilon_{eN}(l, k)]^T.$$

Using (32), we have

$$\xi(l-1, k+1) = (L+B)\tilde{e}(l-1, k+1) \quad (33)$$

We consider two cases: $k=k_i$ and $k_i < k < k_{i+1}$. When $k_i < k < k_{i+1}$, the control input $u_i(l, k)$ of MASs will keep the same value of $u_i(l, k_i)$ such that the closed-loop control of MASs will be broken, and the tracking errors will increase. However, when the tracking error exceeds the triggering condition, the closed-loop control of MASs is recovered. Thus, we only need to discuss the convergence of MASs when $k=k_i$.

Since $\tilde{e}_i(l-1, k+1) = s_i y_0(l-1, k+1) - \tilde{y}_i(l-1, k+1)$, $\tilde{y}_i(l-1, k+1) = \hat{y}_i(l-1, k+1) - g_i(l-1, k+1)$, and $y_0(l, k)$ and $g_i(l, k)$ are constants for all l , we have

$$\tilde{e}_i(l, k+1) = \tilde{e}_i(l-1, k+1) - \Delta \hat{y}_i(l, k+1) \quad (34)$$

where $\Delta \hat{y}_i(l, k+1) = \hat{y}_i(l, k+1) - \hat{y}_i(l-1, k+1)$. Then, according to (2), (15), (16), (33), and (34), we have

$$\begin{aligned} \tilde{e}(l, k+1) &= (I - \beta \Omega(l, k)(L+B))\tilde{e}(l-1, k+1) \\ &\quad - \chi \varepsilon_e(l-1, k+1) \\ &= (I - \beta \psi(l, k))\tilde{e}(l-1, k+1) \\ &\quad - \chi \varepsilon_e(l-1, k+1) \end{aligned} \quad (35)$$

where $\psi(l, k) = \Omega(l, k)(L+B)$, $\Omega(l, k) = \text{diag}(\vartheta_1, \vartheta_2, \dots, \vartheta_N)$, and $0 < \vartheta_i = \frac{\Gamma_i(l, k)\hat{\Gamma}_i(l, k)}{\lambda + |\hat{\Gamma}_i(l, k)|^2} < \frac{\Gamma_i(l, k)}{2\sqrt{\lambda}} < \frac{r}{2\sqrt{\lambda}} < \frac{r}{2\sqrt{\lambda_{\min}}} < 1$. Furthermore, using β , presented in Theorem 3, we have that $I - \beta \psi(l, k)$ is an irreducible substochastic matrix [34]–[36]. From Equation (35), we have

$$\begin{aligned} \|\tilde{e}(l, k+1)\| &\leq \|I - \beta \psi(l, k)\| \cdots \|I - \beta \psi(2, k)\| \|\tilde{e}(1, k+1)\| \\ &\quad + w + \|I - \beta \psi(l, k)\| w + \cdots \\ &\quad + \|I - \beta \psi(l, k)\| \cdots \|I - \beta \psi(3, k)\| w \end{aligned} \quad (36)$$

where $w > \|\chi \varepsilon_e(l-1, k+1)\|$ can be obtained, since χ and $\varepsilon_e(l-1, k+1)$ are bounded. Then, employing Lemma 3, (36) becomes

$$\begin{aligned} \|\tilde{e}(l, k+1)\| &\leq (\lambda^{\lfloor \frac{l-2}{\phi} \rfloor} + \lambda^{\lfloor \frac{l-3}{\phi} \rfloor} + \cdots + \lambda^{\lfloor \frac{0}{\phi} \rfloor}) w \\ &\quad + \lambda^{\lfloor \frac{l-1}{\phi} \rfloor} \|\tilde{e}(l, k+1)\| \end{aligned}$$

Moreover, let $O(l) = \lambda^{\lfloor \frac{l}{\phi} \rfloor} + \lambda^{\lfloor \frac{l+1}{\phi} \rfloor} + \cdots + \lambda^{\lfloor \frac{(l+1)\phi-1}{\phi} \rfloor}$. Then, these can be obtained that $O(l) = \phi \lambda^l$ and

$$\begin{aligned} \lim_{l \rightarrow \infty} \|\tilde{e}(l, k+1)\| &= \lim_{l \rightarrow \infty} (O(l) + O(l-1) + \cdots + O(0)) w \\ &= \lim_{l \rightarrow \infty} (\phi \lambda^l + \phi \lambda^{l-1} + \cdots + \phi) w \\ &= \frac{\phi}{1-\lambda} w \end{aligned} \quad (37)$$

Furthermore, since $\tilde{e}_i(l, k) = s_i y_0(l, k) - \tilde{y}_i(l, k)$ and $e_i(l, k) = s_i y_0(l, k) - y_i(l, k) + g_i(l, k)$, we have

$$e_i(l, k) = \tilde{e}_i(l, k) + \varepsilon_{e_i}(l, k) \quad (38)$$

Hence, according to Theorem 2 and Equations (37) and (38), we have $e_i(l, k)$ is bounded. The designed ET-DMFAILBFC scheme can govern the MASs with a fixed topology to perform time-varying trajectory bipartite formation tracking tasks. ■

Remark 5: From Equations (21), (22), and (38), we can adjust the bounded of the tracking error by changing parameter χ and the dead-zone operator. Hence, the proposed algorithm provides flexibility for the operator by adjusting parameter χ and the dead-zone operator to adapt the requirement of some industrial processes under suitable communication and computation resources. The proposed algorithm will have broader application scenarios.

IV. EXTENSIVE TO TIME-VARYING TOPOLOGIES

Here, the time-varying switching topologies problem for MASs to implement event-triggered bipartite formation tasks is discussed. Moreover, all topologies of MASs are expressed by \bar{G}^p , $p = 1, 2, \dots, \kappa$, and (6) becomes

$$\begin{aligned} \xi_i(l, k) = & \sum_{j \in N_i} (a_{ij}^p(k) \tilde{y}_j(l, k) - |a_{ij}^p(k)| \tilde{y}_i(l, k)) \\ & + b_i^p(k) (s_i^p(k) y_0(l, k) - \tilde{y}_i(l, k)) \end{aligned} \quad (39)$$

Theorem 4: Considering Equation (1) restrained by Assumptions 1-3, the communication graph \bar{G}^p , $p = 1, 2, \dots, \kappa$ restrained by Assumption 4, and employing laws (8)-(10) and (31) with β satisfying

$$\beta < \frac{1}{\max_{i \in S_n, l=1,2,\dots,\kappa} \sum_{j=1}^N |a_{ij}^p(k)| + b_i^p(k)} \quad (40)$$

there is a $\lambda_{\min} > \frac{r^2}{4}$ and $\lambda > \lambda_{\min}$, guaranteeing the boundedness of $\tilde{e}_i(l, k + 1)$.

Proof: According to (39), (35) becomes

$$\begin{aligned} \tilde{e}(l, k + 1) = & (I - \beta \Omega(l, k)(L(k) + B(k))) \\ & \times \tilde{e}(l - 1, k + 1) - \chi \varepsilon_e(l - 1, k + 1) \end{aligned} \quad (41)$$

From (40), we can obtain that the product of β and the arbitrarily diagonal entries of $L(k) + B(k)$ is less than 1. Hence, $I - \beta \psi(l, k)(L(k) + B(k))$ is an irreducible substochastic matrix with positive diagonal entries. According to the analysis process of Theorem 3, we can easily obtain that $\tilde{e}_i(l, k + 1)$ is bounded.

Hence, the proposed ET-DMFAILBFC algorithm also can govern the MASs with switching topologies to perform time-varying trajectory bipartite formation tracking tasks. ■

Remark 6: Most designed bipartite formation algorithms require a precise mathematical model to analyze controlled systems' convergence in the literature. However, during the proof processes of Theorems 3 and 4, we can see that the requirement is not needed in the designed ET-DMFAILBFC algorithm. On the other hand, the existing data-driven ILC schemes [34]–[36] are effective for MASs, but they don't consider the resource-efficient issues, especially combining ILC and event-triggered for MASs.

V. SIMULATION

A. Fixed Topology

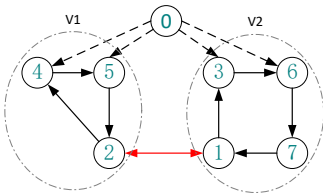


Fig. 2. Communication topology among agents (example 1).

Here, MASs include seven agents. Figure 2 shows the communication topology of the MASs, where the nonlinear dynamics of each agent are considered as

$$y_1(l, k + 1) = \frac{y_1^2(l, k - 1)u_1^2(l, k - 1)}{1 + y_1(l, k - 1)y_1(l, k - 2) + y_1^2(l, k - 3)}$$

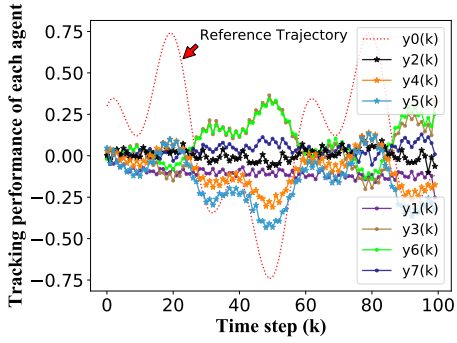
$$\begin{aligned} & + \frac{(1 + (k/165)u_1(l, k - 1))}{1 + y_1(l, k - 1)y_1(l, k - 2) + y_1^2(l, k - 3)} \\ y_2(l, k + 1) = & \frac{y_2^2(l, k - 2)u_2^4(l, k - 2)}{1 + y_2(l, k - 1)y_2(l, k - 2) + y_2^2(l, k - 3)} \\ & + \frac{(1 + (k/165)u_2(l, k - 1))}{1 + y_2(l, k - 1)y_2(l, k - 2) + y_2^2(l, k - 3)} \\ y_3(l, k + 1) = & \frac{y_3^3(l, k - 3)u_3(l, k - 3)}{1 + 2y_3^2(l, k - 3)} \\ & + \frac{(1 + (k/165)u_3^3(l, k - 1))}{1 + 2y_3^2(l, k - 3)} \\ y_4(l, k + 1) = & \frac{y_4^3(l, k - 2)u_4(l, k - 2)}{1 + y_4^2(l, k - 1) + y_4^2(l, k - 2)} \\ & + \frac{(1 + (k/165)u_4(l, k - 1))}{1 + y_4^2(l, k - 1) + y_4^2(l, k - 2)} \\ y_5(l, k + 1) = & \frac{y_5^4(l, k - 2)u_5(l, k - 2)}{1 + 2y_5(l, k - 1)y_5(l, k - 2)} \\ & + \frac{(1 + (k/165)u_5(l, k - 1))}{1 + 2y_5(l, k - 1)y_5(l, k - 2)} \\ y_6(l, k + 1) = & \frac{y_6^4(l, k - 1)u_6(l, k - 2)}{1 + y_6^2(l, k - 1) + y_6^2(l, k - 2)} \\ & + \frac{(1 + (k/165)u_6(l, k - 1))}{1 + y_6^2(l, k - 1) + y_6^2(l, k - 2)} \\ y_7(l, k + 1) = & \frac{y_7^3(l, k - 1)u_7(l, k - 2)}{1 + 2y_7(l, k - 1)y_7(l, k - 2)} \\ & + \frac{(1 + (k/150)u_7^2(l, k - 1))}{1 + 2y_7(l, k - 1)y_7(l, k - 2)} \end{aligned}$$

Remark 7: The dynamics of MASs are heterogeneous, including affine and nonaffine structures. The proposed ET-DMFAILBFC algorithm only uses the above dynamics to generate the I/O data.

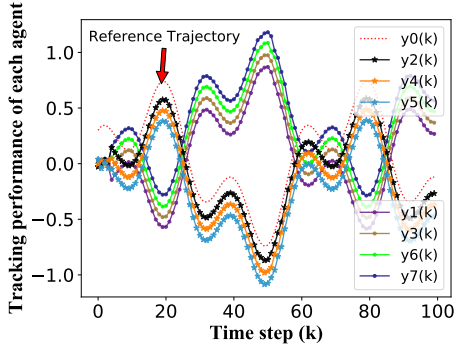
Figure 2 shows that the vertex 0 represents the virtual leader. Agents 2, 4, and 5 consist of the alliance V_1 , and the alliance V_2 is combined with agents 1, 3, 6, and 7. Besides, the collaborative interactions among agents are represented by the solid black line, and the red line represents antagonistic interactions. Moreover, only agents 3, 4, 5, and 6 can acquire data from the virtual leader directly, and the data only flows along the arrow direction, whereas the virtual leader can intervene in the two antagonistic groups by applying the proposed ET-DMFAILBFC scheme. According to the signed graph theory, we obtain that the reciprocal of the greatest diagonal entry of $L + B$ of Fig. 2 is about 0.33. Hence, we set $\beta = 0.24$, which meets the convergence condition of Theorem 3. Moreover, the output of the virtual leader is governed by

$$y_0(l, k) = 0.5 \sin(k\pi/30) + 0.3 \cos(k\pi/10), \quad 0 \leq k \leq 100 \quad (42)$$

The desired formation of this test is designed as $g_1(l, k) = 0.15$, $g_2(l, k) = -0.15$, $g_3(l, k) = 0.25$, $g_4(l, k) = -0.25$, $g_5(l, k) = -0.35$, $g_6(l, k) = 0.35$, and $g_7(l, k) = 0.45$, where $g_i(l, k)$ denotes the desired gap between agent i and the virtual leader, $i = 1, 2, 3, 4, 5, 6, 7$. Initial conditions are set as $u_i(0, k) = 0$, $\hat{\Gamma}_i(0, k) = \hat{\Gamma}_i(1, k) = 2$, and $y_i(l, 0) = \text{rand}[-0.05, 0.05]$ with $k = 1, 2, 3, 4$. Other parameters are selected as $\delta = 0.5$, $\rho = 0.9$, $\lambda = 0.5$, $c = 10^{-4}$, and



(a) Output of the 8th iteration



(b) Output of the 355th iteration

Fig. 3. Output of the MASs with fixed topology (example 1).

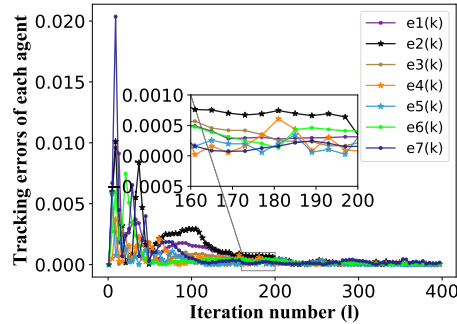


Fig. 4. Tracking errors of MASs with fixed topology (example 1).

$\tau = 10^{-3}$. The simulation results of tracking performances at the 8th iteration and the 355th iteration are presented in Fig. 3. The max bipartite formation tracking errors of each agent are plotted in Fig. 4.

Figures 3-4 show that the vertical intervals among agents are not the same at the beginning iteration, but the differences are reduced dramatically, and the bipartite formation tracking is well achieved after the 200th iteration. Furthermore, Fig. 3.b shows that agents can maintain the desired tracking gap of the counter-trajectory. Figure 5 shows that the event-triggered times of each agent are recorded as 31, 34, 29, 27, 14, 27, 24 at $l = 355$. The average number of the event-triggered is about 26.57, so the designed ET-DMFAILBFC scheme can reduce about 73.43% energy costs of communication and computation for MASs with a fixed communication topology.

Moreover, to further illustrate the advantages of combining

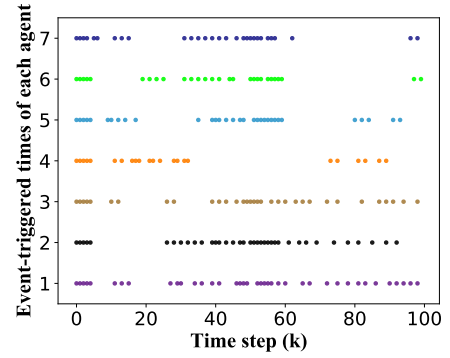


Fig. 5. Even-Triggered signal at the 355th (example 1).

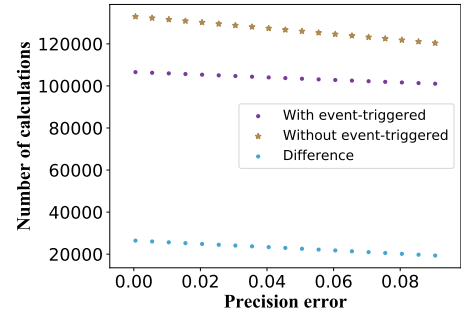


Fig. 6. Calculation numbers for difference scheme (example 1).

the event-triggered mechanism and iterative learning scheme for the designed approach, we have done a contrast experiment shown in Fig. 6, where we can see that the proposed event-triggered iterative method requires fewer computational resources than the iterative method without the event-triggered mechanism.

Remark 8: As we know, the iterative learning method obtains the experiences from past information to improve control performance. If the MASs consist of considerable agents, it is an enormous burden for the calculating unit, which may cause jamming issues for the system operation. According to the proposed event-triggered mechanism, the proposed iterative algorithm will not update the control input if the current tracking error is lower than the event-triggered condition. Hence, it can successfully relieve the memory space and computational burden of the controlled system.

B. Time-varying Switching Topologies

Here, the bipartite formation tracking performance of the MASs with time-varying switching topologies, which are governed by the proposed ETDMFAILBFC algorithm, is presented. All of the parameters are selected the same as in Section V.A, but the communication topologies are changed, which are presented in Fig.7. Moreover, the change law of the topologies is given as the following piecewise function.

$$\begin{cases} \bar{G}^1, & 0 \leq k \leq 30 \\ \bar{G}^2, & 30 < k \leq 60 \\ \bar{G}^3, & 60 < k \leq 100 \end{cases}$$

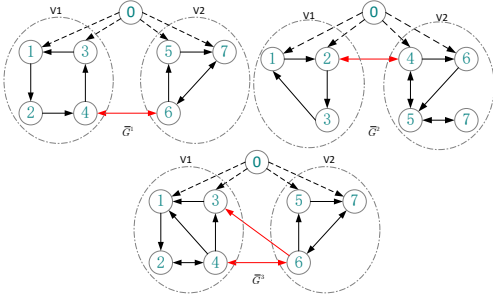


Fig. 7. Time-varying topologies of MASs (example 2).

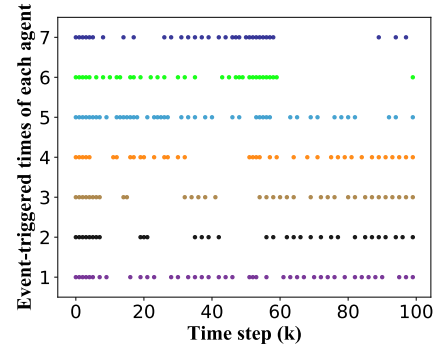
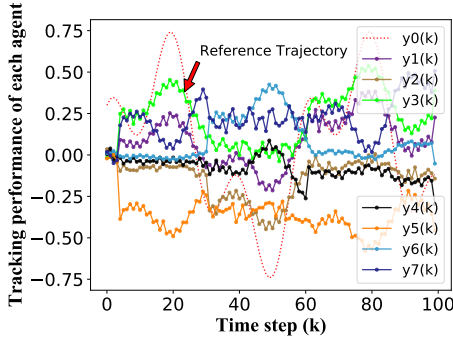
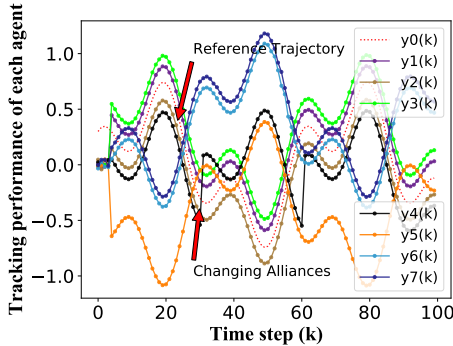


Fig. 10. Even-Triggered signal at the 355th (example 2).



(a) Output of the 8th iteration



(b) Output of the 355th iteration

Fig. 8. Output of the MASs with switching topologies (example 2).

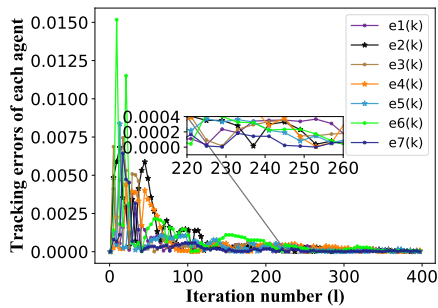


Fig. 9. Tracking errors of each agent (example 2).

From Fig. 8, we see that MASs have a similar performance to the fixed topology results in Fig.3. Also, compared with Fig.4, the bipartite formation tracking errors shown in Fig.9 have a similar convergence property. For example, both of

them converge to a small range around the origin after 245th iterations. The changes of the communication topologies can be seen in Fig. 8.b, where agent 4 betrays its alliance at $k = 30$ and $k = 60$, repetitively. Nevertheless, it is noteworthy that formation tracking performance and event-triggered times only have small differences. The event-triggered times of seven agents are about 44, 37, 39, 32, 43, 30, 34, and the average number of the event-triggered is about 37, shown in Fig. 10. Furthermore, the bipartite formation tracking errors of MASs with switching topologies are presented in Fig. 9, which shows the bipartite formation tracking errors rapidly converge to a small range around zero. Generally, it further verifies the correctness and effectiveness of the designed ET-DMFAILBFC approach.

C. Realistic Direct-current Motors

To verify the proposed ET-DMFAILBFC approach's applicability, we employ seven direct-current motors to implement event-triggered bipartite formation tracking tasks. It is noted that the dynamics of the direct-current motor is identified and investigated in [20], [22], and [34]. The mathematical model is described below.

$$\begin{cases} \dot{x}(t) = \frac{u(t) - f_f(t) - f_r(t)}{m} \\ f_f(t) = f_v \dot{x}(t) \text{sign}(\dot{x}(t)) \\ \quad + \left(f_c + (f_s - f_c) e^{-\left(\dot{x}(t) / \dot{x}_\delta \right)^\delta} \right) \text{sign}(\dot{x}(t)) \\ f_r(t) = o_1 \sin(w_0 x(t)) \\ y(t) = \dot{x}(t) \end{cases} \quad (43)$$

where $\text{sign}(\bullet)$ is the sign function. During the simulation tests, we set $m = 0.59kg$, $\dot{x}_\delta = 0.1$, $\delta = 1$, $f_c = 10N$, $f_s = 20N$, $f_v = 10N \cdot s \cdot m^{-1}$, $o_1 = 8.5N$, and $w_0 = 314s^{-1}$. Furthermore, the objective velocity of the virtual leader is governed the same as in Section V.A. Here, we design the comparative experiments to verify the anti-jamming capability of the designed ET-DMFAILBFC algorithm. One is output measurement without any noise. Another one considers the output with random measurement noise, which is bounded and belongs to $[-0.01, 0.01]$ for each direct-current motor. Here, all parameters and communication topologies are set the same as in Section V.A.

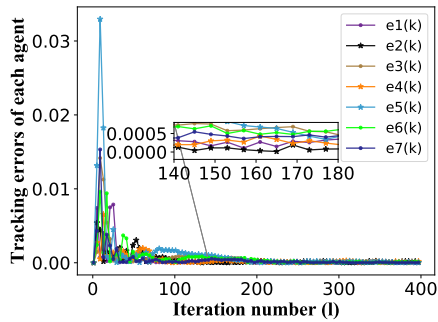


Fig. 11. Tracking errors of each agent without noises (example 3).

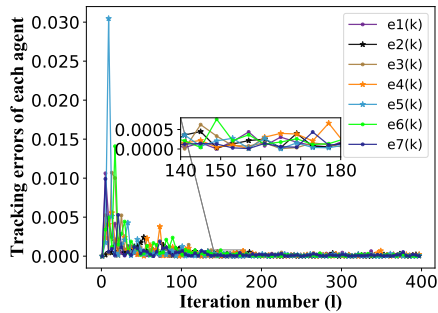


Fig. 12. Tracking errors of each agent with noises (example 4).

From Figs. 11 and 12, we can see both of the situations that the bipartite formation tracking errors dramatically converge to a small range around zero. Moreover, the event-triggered times of seven direct-current motors are shown in Table I.

TABLE I
TRIGGERED NUMBER IN DIFFERENT EXAMPLES

Examples	Triggered Times of All Agents							Average
	1	2	3	4	5	6	7	
1	31	34	29	27	14	27	24	26.57
2	44	37	39	32	43	30	34	37
3	29	24	47	41	30	34	33	34
4	85	78	80	88	87	83	81	83.14

It is noted that random noise is directly added to each direct-current motors’ output, directly affecting the bipartite formation tracking errors and causing the event-triggered times to increase. Fortunately, the designed method has good robustness, where random noises do not destroy the stability of MASs. Our future work will focus on reducing the effect of external disturbance.

Remark 9: Generally, most machines are controlled by direct-current motors, especially for the SISO systems. Therefore, conducting the simulation on the MASs with several direct-current motors is meaningful work.

Remark 10: From the tests, parameters β , λ , and τ affect the convergence of the proposed method. If the value of β is increased without exceeding the requirement of Equation (36), the convergence rate will be increased. Generally, $\lambda \in [1, 100]$ and $\tau < 10^{-3}$. If the control performance is poor, increasing λ and reducing τ are always useful.

VI. CONCLUSION

In this work, an ET-DMFAILBFC algorithm has been formulated for unknown nonaffine nonlinear discrete-time MASs with fixed and time-varying switching topologies. Moreover, an observer-based event-triggering mechanism with a dead-zone operation has been proposed, where both the collaborative and antagonistic interactions among agents are considered. Generally, this scheme is only dependent on each agent’s I/O data and guarantees that all agents can track the desired trajectory with an expected pattern. The convergence of the designed approach has been proved by rigorous mathematical analysis. The corresponding simulations of the designed approach have shown that bipartite formation tracking errors converge to a small range around the origin. Compared with the existing data-driven control algorithms, the proposed algorithm doesn’t need the full I/O data of each agent, which significantly reduces communication and computing consumptions. Our future work will consider the bipartite formation problems for MASs with disturbance and data dropout.

REFERENCES

- [1] H. Liu, T. Ma, F. L. Lewis, and Y. Wan, “Robust formation control for multiple quadrotors with nonlinearities and disturbances,” *IEEE T. Cybern.*, vol. 50, no. 4, pp. 1362–1371, 2018.
- [2] H. Liu, Y. Tian, F. L. Lewis, Y. Wan, and K. P. Valavanis, “Robust formation tracking control for multiple quadrotors under aggressive maneuvers,” *Automatica*, vol. 105, pp. 179–185, 2019.
- [3] T. Menard, S. A. Ajwad, E. Moulay, P. Coirault, and M. Defoort, “Leader-following consensus for multi-agent systems with nonlinear dynamics subject to additive bounded disturbances and asynchronously sampled outputs,” *Automatica*, vol. 121, p. 109176, 2020.
- [4] H. Liu, Y. Wang, F. L. Lewis, and K. P. Valavanis, “Robust formation tracking control for multiple quadrotors subject to switching topologies,” *IEEE Trans. Control Netw. Syst.*, vol. 7, no. 3, pp. 1319–1329, 2020.
- [5] X. Liu, Y. Xie, F. Li, P. Shi, W. Gui, and W. Li, “Formation control of singular multiagent systems with switching topologies,” *Int. J. Robust Nonlinear Control*, vol. 30, no. 2, pp. 652–664, 2020.
- [6] V. P. Tran, M. Garratt, and I. R. Petersen, “Switching time-invariant formation control of a collaborative multi-agent system using negative imaginary systems theory,” *Control Eng. Practice*, vol. 95, p. 104245, 2020.
- [7] Y. Guo, J. Zhou, G. Li, and J. Zhang, “Robust formation tracking and collision avoidance for uncertain nonlinear multi-agent systems subjected to heterogeneous communication delays,” *Neurocomputing*, vol. 395, pp. 107–116, 2020.
- [8] A. González, R. Aragüés, G. López-Nicolás, and C. Sagüés, “Predictor-feedback synthesis in coordinate-free formation control under time-varying delays,” *Automatica*, vol. 113, p. 108811, 2020.
- [9] Y. Wu, J. Hu, Y. Zhang, and Y. Zeng, “Interventional consensus for high-order multi-agent systems with unknown disturbances on competition networks,” *Neurocomputing*, vol. 194, pp. 126–134, 2016.
- [10] K.-K. Oh, M.-C. Park, and H.-S. Ahn, “A survey of multi-agent formation control,” *Automatica*, vol. 53, pp. 424–440, 2015.
- [11] Z. Peng, J. Wang, D. Wang, and Q.-L. Han, “An overview of recent advances in coordinated control of multiple autonomous surface vehicles,” *IEEE Trans. Ind. Inform.*, vol. 17, no. 2, pp. 732–745, 2020.
- [12] A. Dorri, S. S. Kanhere, and R. Jurdak, “Multi-agent systems: A survey,” *IEEE Access*, vol. 6, pp. 28 573–28 593, 2018.
- [13] L. Ding, Q.-L. Han, X. Ge, and X.-M. Zhang, “An overview of recent advances in event-triggered consensus of multiagent systems,” *IEEE T. Cybern.*, vol. 48, no. 4, pp. 1110–1123, 2017.
- [14] X. Ge and Q.-L. Han, “Distributed formation control of networked multi-agent systems using a dynamic event-triggered communication mechanism,” *IEEE Trans. Ind. Electron.*, vol. 64, no. 10, pp. 8118–8127, 2017.
- [15] W. Hu, C. Yang, T. Huang, and W. Gui, “A distributed dynamic event-triggered control approach to consensus of linear multiagent systems with directed networks,” *IEEE T. Cybern.*, vol. 50, no. 2, pp. 869–874, 2018.

- [16] J. Deng, K. Li, S. Wu, and Y. Wen, "Distributed adaptive time-varying formation tracking control for general linear multi-agent systems based on event-triggered strategy," *IEEE Access*, vol. 8, pp. 13 204–13 217, 2020.
- [17] W. Zhu, W. Cao, and Z.-P. Jiang, "Distributed event-triggered formation control of multiagent systems via complex-valued laplacian," *IEEE T. Cybern.*, 2019.
- [18] H.-J. Ma, G.-H. Yang, and T. Chen, "Event-triggered optimal dynamic formation of heterogeneous affine nonlinear multiagent systems," *IEEE Trans. Autom. Control*, vol. 66, no. 2, pp. 497–512, 2020.
- [19] X.-M. Zhang, Q.-L. Han, and B.-L. Zhang, "An overview and deep investigation on sampled-data-based event-triggered control and filtering for networked systems," *IEEE Trans. Ind. Inform.*, vol. 13, no. 1, pp. 4–16, 2016.
- [20] X. Bu, Z. Hou, and H. Zhang, "Data-driven multiagent systems consensus tracking using model free adaptive control," *IEEE Trans. Neural Netw. Learn. Syst.*, vol. 29, no. 5, pp. 1514–1524, 2017.
- [21] S. Xiong, Z. Hou, and S. Jin, "Model-free adaptive formation control for unknown multiinput-multioutput nonlinear heterogeneous discrete-time multiagent systems with bounded disturbance," *Int. J. Robust Nonlinear Control*, vol. 30, no. 15, pp. 6330–6350, 2020.
- [22] H. Zhao, L. Peng, and H. Yu, "Model-free adaptive consensus tracking control for unknown nonlinear multi-agent systems with sensor saturation," *Int. J. Robust Nonlinear Control*, vol. 31, no. 13, pp. 6473–6491, 2021.
- [23] Y. Wang, H. Li, X. Qiu, and X. Xie, "Consensus tracking for nonlinear multi-agent systems with unknown disturbance by using model free adaptive iterative learning control," *Appl. Math. Comput.*, vol. 365, p. 124701, 2020.
- [24] J. Feng, W. Song, H. Zhang, and W. Wang, "Data-driven robust iterative learning consensus tracking control for mimo multiagent systems under fixed and iteration-switching topologies," *IEEE Trans. Syst. Man Cybern.-Syst.*, 2020.
- [25] H. Zhao, L. Peng, and H. Yu, "Quantized model-free adaptive iterative learning bipartite consensus tracking for unknown nonlinear multi-agent systems," *Appl. Math. Comput.*, vol. 412, p. 126582, 2022.
- [26] C. L. Remes, R. B. Gomes, J. V. Flores, F. B. Lbano, and L. Campestrini, "Virtual reference feedback tuning applied to dc–dc converters," *IEEE Trans. Ind. Electron.*, vol. 68, no. 1, pp. 544–552, 2020.
- [27] Y. Lu, G. Zhang, L. Qiao, and W. Zhang, "Adaptive output-feedback formation control for underactuated surface vessels," *Int. J. Control*, vol. 93, no. 3, pp. 400–409, 2020.
- [28] Y. Lin, M. Wang, X. Zhou, G. Ding, and S. Mao, "Dynamic spectrum interaction of uav flight formation communication with priority: A deep reinforcement learning approach," *IEEE Trans. Cogn. Commun. Netw.*, vol. 6, no. 3, pp. 892–903, 2020.
- [29] G. Wen, C. P. Chen, and B. Li, "Optimized formation control using simplified reinforcement learning for a class of multiagent systems with unknown dynamics," *IEEE Trans. Ind. Electron.*, vol. 67, no. 9, pp. 7879–7888, 2019.
- [30] H. Jiang and H. He, "Data-driven distributed output consensus control for partially observable multiagent systems," *IEEE T. Cybern.*, vol. 49, no. 3, pp. 848–858, 2018.
- [31] Y. Hui, R. Chi, B. Huang, and Z. Hou, "3-d learning-enhanced adaptive ilc for iteration-varying formation tasks," *IEEE Trans. Neural Netw. Learn. Syst.*, vol. 31, no. 1, pp. 89–99, 2019.
- [32] H.-S. Ahn and Y. Chen, "Iterative learning control for multi-agent formation," in *2009 ICCAS-SICE*. IEEE, 2009, pp. 3111–3116.
- [33] A. Polyakov, D. Efimov, and W. Perruquetti, "Robust stabilization of mimo systems in finite/fixed time," *Int. J. Robust Nonlinear Control*, vol. 26, no. 1, pp. 69–90, 2016.
- [34] X. Bu, Q. Yu, Z. Hou, and W. Qian, "Model free adaptive iterative learning consensus tracking control for a class of nonlinear multiagent systems," *IEEE Trans. Syst. Man Cybern.-Syst.*, vol. 49, no. 4, pp. 677–686, 2017.
- [35] X. Bu, L. Cui, Z. Hou, and W. Qian, "Formation control for a class of nonlinear multiagent systems using model-free adaptive iterative learning," *Int. J. Robust Nonlinear Control*, vol. 28, no. 4, pp. 1402–1412, 2018.
- [36] R. Chi, Y. Hui, B. Huang, and Z. Hou, "Adjacent-agent dynamic linearization-based iterative learning formation control," *IEEE T. Cybern.*, vol. 50, no. 10, pp. 4358–4369, 2019.
- [37] C. Altafini, "Consensus problems on networks with antagonistic interactions," *IEEE Trans. Autom. Control*, vol. 58, no. 4, pp. 935–946, 2012.
- [38] J. Duan, H. Zhang, J. Han, and Z. Gao, "Bipartite output consensus of heterogeneous linear multi-agent systems by dynamic triggering observer," *ISA Trans.*, vol. 92, pp. 14–22, 2019.
- [39] H. Zhang, Y. Cai, Y. Wang, and H. Su, "Adaptive bipartite event-triggered output consensus of heterogeneous linear multiagent systems under fixed and switching topologies," *IEEE Trans. Neural Netw. Learn. Syst.*, vol. 31, no. 11, pp. 4816–4830, 2020.
- [40] C. Zong, Z. Ji, L. Tian, and Y. Zhang, "Distributed multi-robot formation control based on bipartite consensus with time-varying delays," *IEEE Access*, vol. 7, pp. 144 790–144 798, 2019.
- [41] W. Wang, C. Huang, C. Huang, J. Cao, J. Lu, and L. Wang, "Bipartite formation problem of second-order nonlinear multi-agent systems with hybrid impulses," *Appl. Math. Comput.*, vol. 370, p. 124926, 2020.
- [42] Y. Wang and M. Hou, "Model-free adaptive integral terminal sliding mode predictive control for a class of discrete-time nonlinear systems," *ISA Trans.*, vol. 93, pp. 209–217, 2019.
- [43] D. Zhao, T. Dong, and W. Hu, "Event-triggered consensus of discrete time second-order multi-agent network," *Int. J. Control Autom. Syst.*, vol. 16, no. 1, pp. 87–96, 2018.
- [44] S. Yang, J.-X. Xu, and X. Li, "Iterative learning control with input sharing for multi-agent consensus tracking," *Syst. Control Lett.*, vol. 94, pp. 97–106, 2016.



Huarong Zhao received the M.S. degree in mechatronic engineering from Guilin University of Electronic Technology, Guilin, China, in 2018. He is currently working toward the Ph.D. degree at the School of Internet of Things Engineering in Jiangnan University, Wuxi, China and is a visiting scholar of York University, Toronto ON, Canada. His research interests include multi-agent systems, reinforcement learning, and image processing.



Hongnian Yu (IoT Fellow, IEEE Senior Member) is the Smart Technology Research Centre Director the Head of Research with the School of Engineering and the Built Environment, Edinburgh Napier University. His research covers the two main areas: 1) robotics with applications in the rescue and recovery operations, and healthcare and 2) ICT enabled healthcare including assistive technologies in supporting elderly and people with dementia, and activity recognition of elderly people. He has published over 200 journal and conference research papers. He is a member of the EPSRC-Peer Review College and a Fellow of IET and RSA. He has held several research grants worth about ten million pounds from the U.K., EPSRC, the Royal Society, and the European, as well as from industry. He was awarded the F.C. William Premium for his paper on adaptive and robust control of robot manipulators by the IEE Council, and has won the Gold Medal on The World Exhibition on Inventions, Research, and New Technologies, INNOVA 2009, Brussels, the International Exhibition of Inventions, Geneva, Switzerland, in 2010, for the invention "Method and device for driving mobile inertial robots"; and the 43rd International Exhibition of Inventions, New Techniques, and Products, Geneva, in 2015.



Li Peng received the Ph.D. degree from the School of Information Engineering, University of Science and Technology, Beijing, in 2002. He is currently a Professor at the School of Internet of Things Engineering, Jiangnan University, Wuxi, China. He is a member of the Chinese Computer Association, and also Chinese Artificial Intelligent Association. His research interests are computer simulation, intelligent control and visual wireless sensor network.